Magnetoelastic effects in terbium ferroborate

Cite as: Low Temp. Phys. **34**, 901 (2008); https://doi.org/10.1063/1.3009584
Published Online: 13 November 2008

G. A. Zvyagina, K. R. Zhekov, L. N. Bezmaternykh, I. A. Gudim, I. V. Bilych, and A. A. Zvyagin

Magnetoelastic effects in terbium ferroborate

G. A. Zvyagina[a] and K. R. Zhekov

B. I. Verkin Institute for Low-Temperature Physics and Engineering of the National Academy of Sciences of Ukraine, pr. Lenina 47, Kharkov 61103, Ukraine

L. N. Bezmaternykh and I. A. Gudim

L. V. Kirenskiĭ Institute of Physics of the Siberian Branch of the Russian Adcademy of Sciences, Krasnoyarsk 660036, Russia

I. V. Bilych and A. A. Zvyagin

B. I. Verkin Institute for Low-Temperature Physics and Engineering of the National Academy of Sciences of Ukraine, pr. Lenina 47, Kharkov 61103, Ukraine

(Submitted June 20, 2008)
Fiz. Nizk. Temp. **34**, 1142–1151 (2008)

The behavior of the elastic moduli and sound absorption in a terbium orthoborate single crystal at low temperatures is studied. The components of the tensor of the elastic moduli of this system are determined. A structural phase transition and a transition of the magnetic subsystem into an antiferromagnetically ordered state appear in the temperature dependences of the sound velocities and absorption. The magnetic field dependences of the velocities of transverse sound exhibit singularities in the form of jumps at a magnetic field equal to the field of the spin-flop transition of the antiferromagnetic subsystem. Theoretical analysis shows that the observed behavior of the acoustic characteristics are associated not with the rare-earth subsystem of ferroborate but rather with the renormalization of the exchange interaction between iron ions as a result of the magnetoelastic coupling. © *2008 American Institute of Physics*. [DOI: 10.1063/1.3009584]

I. INTRODUCTION

The family of crystals $RM_3(BO_3)_4$, where R=Y or a rare-earth ion and M=Al, Ga, Sc, Cr, or Fe, is attracting the attention of researchers for a number of reasons. Different combinations of R and M lead to a wide diversity of physical properties, which, combined with thermal and chemical stability, make these crystals extremely interesting for fundamental physics as well as for practical applications. For example, because of their specific optical properties Nd-doped $Y(Gd)Al_3(BO_3)_4$ crystals are used in laser technology for generating radiation at the fundamental frequency and the second harmonic frequency.[1,2]

Rare-earth borates containing a magnetic iron ion demonstrate interesting magnetic properties because of the presence of two different forms of the magnetic ions (3*d* and 4*f* elements).[3,4] These properties are due to the specific behavior of the iron magnetic subsystem, the characteristics of the crystal-field induced electronic structure of the rare-earth ion, and the *f-d* interaction. The competition between the contributions of these two subsystems to the formation of the magnetic structure presupposes the existence of transitions occurring with a change in temperature as well as the magnetic field. Investigations of the magnetic structures in crystals belonging to this group have revealed a wide range of possible states: depending on the type of rare-earth ion, these compounds can be easy-axis or easy-plane antiferromagnets as well as spiral magnets or they can form canted magnetic structures.

For certain ferroborates (R=Gd,Nd) a correlation has been established between the magnetoelastic and magnetoelectric properties.[5,6] This has enabled the authors of these works to classify these compounds as multiferroics, i.e. materials in which two of the three order parameters coexist: elastic, electric, or magnetic. Multiferroelectric effects are most strongly manifested in spontaneous and magnetic-field-induced phase transitions.

This is why it is of interest to study the elastic properties of these compounds near the structural and magnetic phase transitions. The present work is devoted to an investigation of the elastic properties as well as magnetoelastic effects in terbium ferroborate ($TbFe_3(BO_3)_4$).

II. STRUCTURE AND MAGNETIC PROPERTIES OF $TbFe_3(BO_3)_4$

At room temperature $TbFe_3(BO_3)_4$, like all crystals of this family, possesses trigonal (rhombohedral) crystal-lattice symmetry (space group $R32$ (D_3^7) and the structure of the mineral hantite $CaMg_3(CO_3)_4$.[7] The unit cell contains one formula unit. Characteristic structural features are helicoidal chains, oriented along with the trigonal axis *c*, which are connected along the edges of FeO_6 octahedra. Three such chains are coupled with one another by triangular prisms TbO_6 and equilateral triangles BO_3 unite the iron chains into a single three-dimensional structure. In addition, equilateral BO_3 triangles couple TbO_6 prisms and two FeO_6 octahedra, belonging to different chains. The FeO_6 octahedra in the *ab* plane lie at the vertices of an equilateral triangle. A first-order structural phase transition occurs in the crystal at temperature T_c=192 K (Ref. 9) (according to data presented in the review Ref. 8, 290 K and 196 K). As a result of this transition, one of the chains shifts along the *c* axis with respect to the other two chains, which results in the appearance

TABLE I. Absolute values of the sound velocities measured at 77 K and the elastic moduli of $TbFe_3(BO_3)_4$.

Wave vector **q**	ρs_2	$S(\mathbf{m}, \mathbf{n})$	$S \cdot 10^5$ cm/s	C, 10^{11}, dynes/cm^2
[100]	C_{11}	$S(x, x)$	7.6	27.2
	$0.5\{C_{44}+C_{66}+[(C_{66}-C_{44})^2+4C_{14}^2]^{1/2}\}$	$S(x, y)$	3.8	6.8
	$0.5\{C_{44}+C_{66}-[(C_{66}-C_{44})^2+4C_{14}^2]^{1/2}\}$	$S(x, z)$	3.16	4.7 $C_{14}=4.76$
[010]	$0.5\{C_{11}+C_{44}+[(C_{11}-C_{44})^2+4C_{14}^2]^{1/2}\}$	$S(y, y)$	7.75	28.3
	$C_{66}=(C_{11}-C_{12})/2$	$S(y, x)$	3.99	7.5 $C_{12}=12.2$
	$0.5\{C_{11}+C_{44}-[(C_{11}-C_{44})^2+4C_{14}^2]^{1/2}\}$	$S(y, z)$	3.7	6.45
[001]	C_{33}	$S(z, z)$	6.7	21.1
	C_{44}	$S(z, x)$	4.0	7.54
	C_{44}	$S(z, y)$	4.0	7.54

of two nonequivalent positions of iron. The transition is accompanied by a lowering of the local symmetry of the rare-earth ion from D_3 at $T>T_c$ to C_2 ($T<T_c$). Thus, as a result of the structural transition, the unit cell of this compound remains trigonal: the symmetry space group is $R32$ at $T>T_c$ and $P3_121$ at $T<T_c$.[9] The unit cell of the low-temperature phase contains three formula units.

Antiferromagnetic ordering of the iron subsystem occurs in all compounds of this family at low temperatures (20 K $<T_N<$ 40 K). In the literature, there are two viewpoints concerning the fate of the rare-earth subsystem. According to the works analyzed in the review Ref. 8, the rare-earth subsystem, remaining paramagnetic down to the lowest temperatures, becomes magnetized by the magnetic field of the ordered iron subsystem. The antiferromagnetic transition temperature $T_N=20-40$ K depends only slightly on the form of the rare-earth ion but the R^{3+} ions determine the orientation of the magnetic moments of the Fe^{3+} ions in the ordered state. For example, the magnetic moments of iron in compounds with Y, Nd, Er, and Tm are oriented in the *ab* plane, while in the compounds with Tb and Dy they are parallel to the *c* axis. On the other hand, studying the magnetic properties and performing an experiment on neutron diffraction by compounds with Tb, the authors of Ref. 10 suppose that antiferromagnetic ordering of the helicoidal chains of iron ions arises at 40 K and that magnetic ordering of the Tb ions arises at the same temperature and results in antiparallel orientation of the magnetic moments of the Fe and Tb ions in the *ab* plane at 2 K.

III. EXPERIMENTAL RESULTS

Isometric $TbFe_3(BO_3)_4$ single crystals grown from a fluxed solution based on bismuth trimolybdate by the procedure described in Ref. 11 reached sizes up to 10–12 mm. We investigated a crystal which consisted of a transparent green plate less than 1 mm thick in a direction close to the three-fold axis of symmetry. Samples with the characteristic dimensions $\sim 0.5\times1\times1$ mm were prepared from it.

The backward x-ray reflection method (the Laue method) was used to orient the samples. Measurements using the "nonius" procedure[12] were performed to obtain absolute sound velocities with adequate accuracy ($\sim 1\%$). This procedure consists in determining the integral number of wavelengths n which fit within the sample according to the slope of its phase-frequency characteristic. The phase-frequency characteristics were measured in the range 53–55 MHz. The sound velocity obtained in this manner was then refined using the real phase shift $\Phi=2n\pi+\delta\Phi$ due to the sample ($\delta\Phi<2\pi$ is the phase shift recorded with a phase meter).

The tensor of the elastic moduli of the trigonal group contains six independent components: C_{11}, C_{33}, C_{44}, C_{66}, C_{13}, and C_{14}. The values of the elastic constants $C=\rho s^2$, where $\rho=4.71$ g/cm^3 is the density of the material and s are the absolute values of the velocities of longitudinal and transverse sound waves propagating along the **x**, **y**, and **z** axes of a standard, for a trigonal crystal, Cartesian coordinate system ($\mathbf{y}\|C_2$ and $\mathbf{z}\|C_3$), were calculated using the relations presented in Table I. The value of the modulus C_{13} was not calculated, since it was impossible to measure the required sound velocities in the available samples.

The absolute values of the sound velocities measured at the temperature of liquid nitrogen and the computed values of the elastic constants Table I. Here and below, as a simpli-

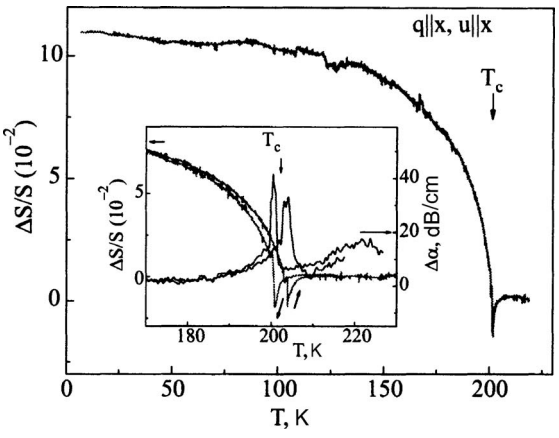

FIG. 1. Temperature dependence of the velocity and absorption of the sound mode C_{11}.

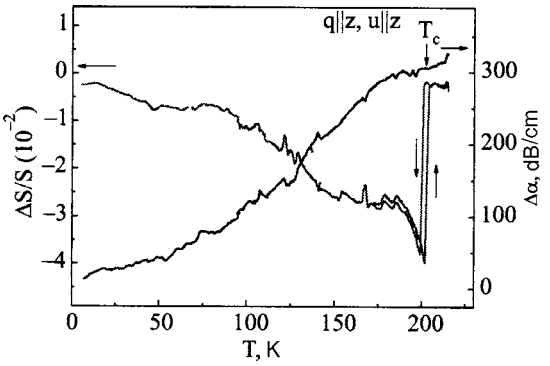

FIG. 2. Temperature dependence of the velocity and absorption of the sound mode C_{33}.

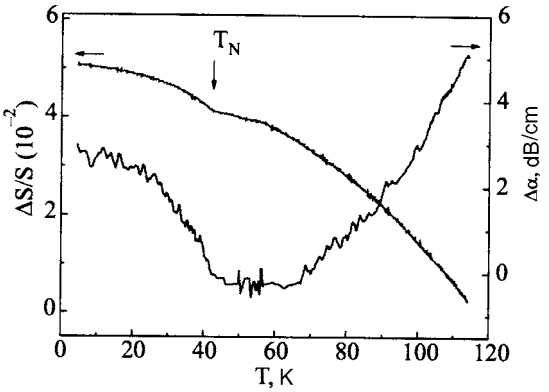

FIG. 3. Temperature dependence of the velocity and absorption of the sound wave ($\mathbf{q}\|\mathbf{x},\mathbf{u}\|\mathbf{z}$).

fication, the following notation is introduced: $S(\mathbf{m},\mathbf{n})$ is the velocity of a sound waves in which the wave vector $\mathbf{q}$ is parallel to the direction $\mathbf{m}$, the displacement vector $\mathbf{u}$ of the particles in the sound wave is oriented in the direction $\mathbf{n}$ ($\mathbf{m},\mathbf{n}=\mathbf{x},\mathbf{y},\mathbf{z}$).

The measurements of the relative changes of the sound velocity and damping were also performed using the automated apparatus described in Ref. 12. The accuracy of the relative measurements for ~0.5 mm thick samples was $\sim 10^{-4}$ for the velocity and ~0.05 dB for the damping. The temperature range was 1.7–300 K, the magnetic fields reached 50 kOe, and the working frequency was 54.3 MHz.

A. Temperature dependences of the sound velocity and absorption

As temperature decreases from 300 K, jumps are observed in the temperature dependences of the velocities of longitudinal and transverse sound modes near 200 K. This attests to the presence of a structural transformation in this compound. The temperatures at which the features are observed depend on the direction of the temperature scan and differ by approximately 1 K. We determined the value of the critical temperature T_c=201 K as the average between the temperatures at which the singularities are observed on heating and cooling. Examples of dependences for longitudinal velocities, corresponding to the sound modes C_{11} and C_{33}, are presented in Figs. 1 and 2. The jump-like behavior of the longitudinal and transverse sound modes near T_c and the presence of temperature hysteresis make it possible to classify this transformation as a first-order structural phase transition. Our result agrees well with existing data showing that such a phase transition does indeed occur in this compound. The value obtained for the critical transition temperature in our experiment differs somewhat from the published values (192, 198, and 240 K (Refs. 8 and 9)); this difference is probably due to the fact that the single crystals were grown by different methods.

As temperature decrease further, right down to the lowest temperature of the experiment 1.7 K, we recorded the temperature behavior of the longitudinal and transverse sound modes that is typical for solids with no anomalies. The temperature dependences of the velocities of the sound waves ($\mathbf{q}\|\mathbf{x},\mathbf{u}\|\mathbf{z}$) and ($\mathbf{q}\|\mathbf{y},\mathbf{u}\|\mathbf{z}$) are exceptions. These modes demonstrate weak singularities, which can be interpreted as kinks (or weak jumps superposed on the variation as a function of temperature) at 40 K (see, for example, Fig. 3, which displays the velocity and damping of the sound wave ($\mathbf{q}\|\mathbf{x},\mathbf{u}\|\mathbf{z}$) as a function of temperature). The information showing that a transition into the antiferromagnetic ordered state occurs in the compound $TbFe_3(BO_3)_4$ at this temperature (according to magnetic measurements performed in Ref. 10) makes it possible to associate the observed features precisely to the Néel point.

B. Magnetic field dependences of the sound velocity and absorption

The magnetic-field dependences of the sound velocity and absorption at fixed temperatures were measured up to 50 K for two mutually perpendicular directions of the external magnetic field (directed along the three-fold symmetry axis $\mathbf{z}$ and in the basal plane). For $\mathbf{H}\|\mathbf{z}$ all transverse velocities studied for a definite value of the magnetic field H_{SF} (the value of H_{SF} varies with temperature) decrease abruptly (the magnitude of the jump ranges from 0.2 to 3% for different modes). The jump in the sound velocity is accompanied by an absorption anomaly. Examples of magnetic-field dependences of the transverse velocities and absorption of sound are presented in Figs. 4–8. A temperature increase essentially has no effect on the magnitude of the jump in the velocity and simply shifts the jump in the direction of higher fields (Figs. 4 and 6). A deviation of the vector $\mathbf{H}$ away from the $\mathbf{z}$ axis at a fixed temperature likewise shifts the jump in the direction of higher fields, but the magnitude of the jump

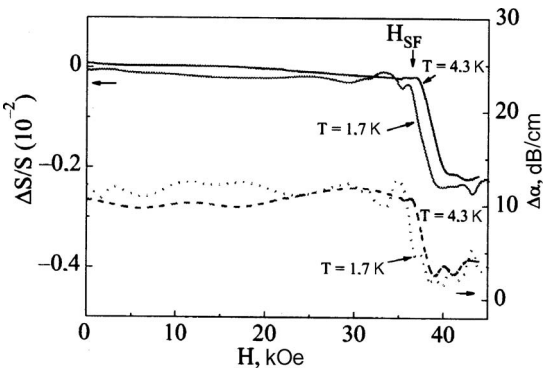

FIG. 4. Magnetic field dependence of the velocity (solid curves) and absorption (dashed curve) of the sound wave ($\mathbf{q}\|\mathbf{x},\mathbf{u}\|\mathbf{z}$) at temperatures 1.7 K and 4.3 K, $\mathbf{H}\|\mathbf{z}$.

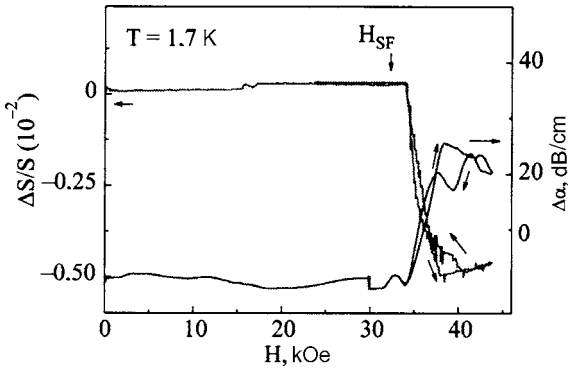

FIG. 5. Magnetic field dependence of the velocity and absorption of the sound wave ($\mathbf{q}\|\mathbf{y},\mathbf{u}\|\mathbf{z}$) at temperature 1.7 K, $\mathbf{H}\|\mathbf{z}$.

decreases with increasing angle (Figs. 7 and 8). However, when the vector **H** lies in the basal plane, the sound velocity and absorption do not show any anomalies right up to the maximum field 50 kOe in our experiment.

Of interest is the fact that the strongest hysteresis with increasing and decreasing magnetic field is observed for the sound velocity and absorption of the modes C_{44} and C_{66} (Figs. 6 and 7). This hysteresis in the behavior of the sound velocity remains for small ($\sim 5°$) deviations of the direction of the magnetic field away from the **z** axis and with decreasing magnitude of the jump with increasing angle (Fig. 7a). As far as the behavior of sound absorption is concerned, as the angle of deviation increases, the form of the singularity changes substantially starting at small values of the angle (Fig. 7b).

We note that the magnetic field behavior of the elastic moduli C_{44} and C_{66} demonstrates a loop feature in fields above the field at which a velocity jump was observed (Figs. 6 and 7).

Of the three longitudinal modes the velocities of the sound waves ($\mathbf{q},\mathbf{u}\|\mathbf{x}$) and ($\mathbf{q},\mathbf{u}\|\mathbf{y}$) demonstrate very weak features (jumps less than 0.1%) in the magnetic field dependences for $\mathbf{H}\|\mathbf{x}$ (Fig. 9). These anomalies are much weaker than for transverse modes.

The critical fields of these singularities which we observed in the behavior of sound modes and the corresponding temperatures correlate well with the values of the fields and

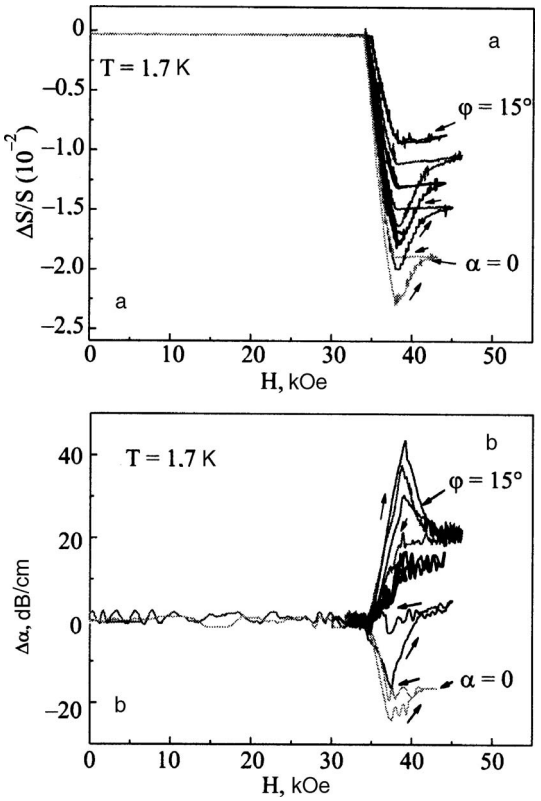

FIG. 7. Magnetic field dependence of the velocity (a) and absorption (b) of the sound wave ($\mathbf{q}\|\mathbf{y},\mathbf{u}\|\mathbf{x}$) at temperature 1.7 K inclination of the direction of the external magnetic field away from the **z** axis carrying with step 3° in the range 0–15°.

temperatures for which, according to the magnetic measurements performed in Ref. 10, a spin-reorientation phase transition of the spin-flop type occurs in the compound $TbFe_3(BO_3)_4$.

IV. DISCUSSION

The changes, which we measured, in the sound velocities and absorption are associated with the elastic, magnetoelastic, and magnetic subsystems of the substance being studied. In terbium ferroborate the magnetic subsystem consists of iron and terbium ions. The magnetic interactions in the experimental material can be classified according to their

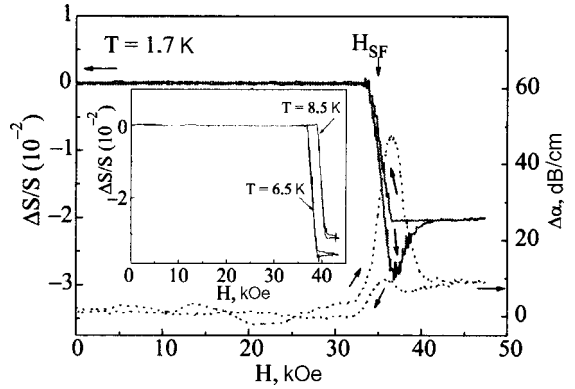

FIG. 6. Magnetic field dependence of the velocity (solid curves) and absorption (dashed curves) of the sound wave ($\mathbf{q}\|\mathbf{z},\mathbf{u}\|\mathbf{x}$) at temperature 1.7 K, $\mathbf{H}\|\mathbf{z}$. Inset: Magnetic field dependence of the velocity of the same mode at temperatures 6.5 and 8.5 K.

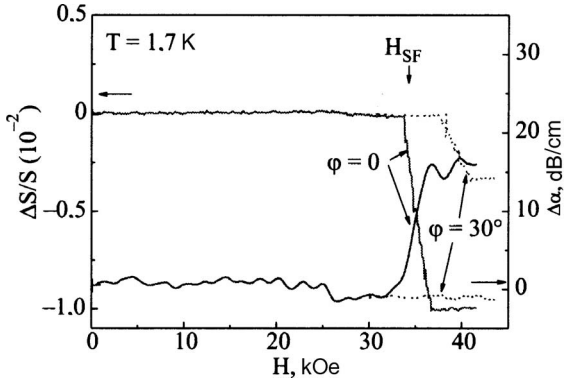

FIG. 8. Magnetic field dependence of the velocity and absorption of the sound wave ($\mathbf{q}\|\mathbf{x},\mathbf{u}\|\mathbf{y}$) at temperature 1.7 K. φ—angle of inclination of the direction of the external magnetic field away from the **z** axis; φ=0° (solid curves) and φ=30° (dashed curves).

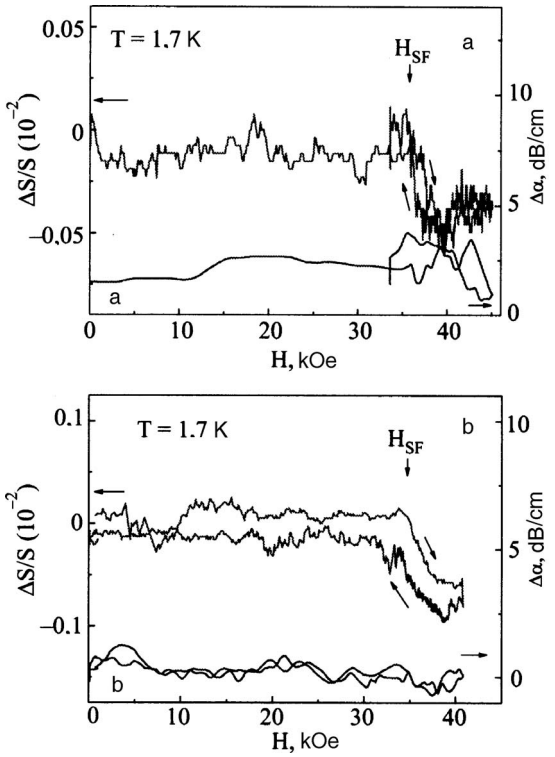

FIG. 9. Magnetic field dependences of the velocity and absorption of longitudinal sound waves: (a) $(\mathbf{q},\mathbf{u}\|\mathbf{x})$ at temperature 1.7 K, $\mathbf{H}\|\mathbf{z}$; (b) $(\mathbf{q},\mathbf{u}\|\mathbf{y})$ at temperature 1.7 K, $\mathbf{H}\|\mathbf{z}$.

strength in decreasing order. The main interaction which determines the presence of magnetic order in the system is the exchange interaction of the iron ions with one another. Iron and terbium ions interact with one another via the weaker *f-d* exchange. As for relativistic interactions, iron ions in ferroborate at low temperatures are in a singlet orbital state, so that single-ion magnetic anisotropy is negligibly small for these ions. For terbium ions, conversely, the strong spin-orbit coupling results in large magnetic anisotropy of the easy-axis type, with the easy axis oriented along the *c* axis of the crystal. The weakest magnetic interaction in the system is the magnetic-dipole interaction.

In ferroborate, the magnetic subsystem can interact with the elastic subsystem by means of two basic mechanisms. In the first place, a change of the positions of the nonmagnetic environment of magnetic ions (ligands) as a result of an interaction with sound can change the electric fields of the ligands, which, because of the spin-orbit coupling, can change the magnitude of the single-ion magnetic anisotropy of terbium ions. In the second place, elastic strain can change the degree of overlapping of the wave functions of the ions participating in exchange, which will change the effective exchange integrals between iron ions. It seems to us that in the leading approximation the effect of sound waves on the essentially local exchange interaction between iron and terbium ions can be neglected. We shall analyze systematically how these possible mechanisms are realized in terbium ferroborate, relying on the results of our measurements of the variation of the sound velocities and absorption as a function of temperature and external magnetic field.

The first mechanism, i.e. the effect of the magnetoelastic interaction on the single-ion magnetic anisotropy of terbium ions, was examined theoretically in Ref. 13, where the possible magnetostriction in ferroborates was investigated. The behavior of the elastic subsystem in a trigonal crystal is associated with the behavior of six elastic moduli which are related with the measured sound velocities by the following relations.

1. The direction of propagation of sound along the **z** axis (three-fold symmetry axis)

$$\rho s_1^2 = \frac{1}{3}(C^{\alpha 1} + 2C^{\alpha 2} + 2\sqrt{2}C^{\alpha 12})$$

—longitudinal wave;

$$\rho s_{2,3}^2 = \frac{1}{2}C^{\xi}$$

—two transverse waves.

2. Direction of sound propagation along the **x** axis

$$\rho s_1^2 = \frac{1}{3}\left(C^{\alpha 1} + \frac{1}{2}C^{\alpha 2} - 2\sqrt{2}C^{\alpha 12}\right) + \frac{1}{2}C^{\varepsilon}$$

—longitudinal wave;

$$\rho s_{2,3}^2 = \frac{1}{4}C^{\varepsilon} + \frac{1}{4}C^{\xi} \pm \frac{1}{4}\sqrt{2(C^{\varepsilon} - C^{\xi})^2 + 16(C^{\varepsilon\xi})^2}$$

—two transverse waves.

3. Direction of sound propagation along the **y** axis (two-fold symmetry axis)

$$\rho s_{1,2}^2 = \frac{1}{6}C^{\alpha 1} + \frac{1}{12}C^{\alpha 2} - \frac{\sqrt{2}}{3}C^{\alpha 12} + \frac{1}{4}C^{\varepsilon} + \frac{1}{4}C^{\xi}$$
$$\pm\frac{1}{2}\sqrt{\left(\frac{1}{6}C^{\alpha 1} + \frac{1}{12}C^{\alpha 2} - \frac{\sqrt{2}}{3}C^{\alpha 12} + \frac{1}{4}C^{\varepsilon} - \frac{1}{4}C^{\xi}\right)^2 + 4(C^{\varepsilon\xi})^2}$$

(+)—quasilongitudinal wave, (−)—quasitransverse wave,

$$\rho s_3^2 = \frac{1}{2}C^{\varepsilon}$$

—transverse wave.

4. Direction of sound propagation in the *yz* plane at an angle of 45° to the **z** axis

$$\rho s_{1,2}^2 = \frac{1}{4}\left(\frac{2}{3}C^{\alpha 1} + \frac{5}{6}C^{\alpha 2} + \frac{1}{2}C^{\varepsilon} + C^{\xi} + 2C^{\varepsilon\xi}\right)$$
$$\pm\frac{1}{4}\sqrt{\left(-\frac{1}{2}C^{\alpha 2} - \frac{4\sqrt{2}}{3}C^{\alpha 12} + \frac{1}{2}C^{\varepsilon} + C^{\varepsilon\xi}\right)^2 + \left(\frac{2}{3}C^{\alpha 1} - \frac{2}{3}C^{\alpha 2} - \frac{2\sqrt{2}}{2}C^{\alpha 12} + C^{\varepsilon} + 2C^{\varepsilon\xi}\right)^2}$$

(+)—quasilongitudinal wave, (−)—quasitransverse wave,

$$\rho s_3^2 = \frac{1}{4}C^{\varepsilon} + \frac{1}{4}C^{\xi} - C^{\varepsilon\xi}$$

—transverse wave,

where $C^{\alpha 1}$, $C^{\alpha 2}$, $C^{\alpha 12}$, C^{ε}, C^{ξ}, and $C^{\varepsilon\xi}$ are the six elastic moduli of a trigonal crystal written in terms of the normal coordinates for this system. The standard elastic moduli which we mentioned previously are related with these moduli by the following relations:

$$\begin{aligned}
C_{11} &= \frac{1}{3}(C^{\alpha 1} + \frac{1}{2}C^{\alpha 2} - 2\sqrt{2}C^{\alpha 12}) + \frac{1}{2}C^{\varepsilon};\\
C_{12} &= \frac{1}{3}(C^{\alpha 1} + \frac{1}{2}C^{\alpha 2} - 2\sqrt{2}C^{\alpha 12}) - \frac{1}{2}C^{\varepsilon};\\
C_{33} &= \frac{1}{3}(C^{\alpha 1} + 2C^{\alpha 2} + 2\sqrt{2}C^{\alpha 12});\\
C_{13} &= \frac{1}{3}(C^{\alpha 1} - C^{\alpha 2} + \frac{\sqrt{2}}{2}C^{\alpha 12});\\
C_{14} &= -C^{\varepsilon\xi};\\
C_{44} &= \frac{1}{2}C^{\xi};\\
C_{66} &= \frac{1}{2}C^{\varepsilon}.
\end{aligned} \tag{1}$$

The authors of Ref. 13 assumed the existence of a coupling between the elastic subsystem of ferroborates and the magnetic single-ion anisotropy of rare-earth ions. In accordance with these calculations, the strongest changes should be manifested in the temperature behavior of the elastic moduli (3)$C^{\alpha 1}$, $C^{\alpha 2}$, and $C^{\alpha 12}$ (see Eq. (16) and Fig. 3 of Ref. 13). As follows from the relations (1), in accordance with these results the strongest temperature should be observed in the longitudinal sound velocities C_{33} and C_{11}, and the transverse modes should change more weakly. However, the strong changes predicted for longitudinal sound by the theory of Ref. 13 are not observed experimentally (Figs. 1 and 2). In addition, as one can see in Figs. 1–3, the changes occurring in the longitudinal and transverse elastic moduli in the temperature range predicted in Ref. 13 are of the same order of magnitude. This probably means that the authors of Ref. 13 used values of the magnetoelastic coupling constants between the lattice vibrations and magnetic single-ion anisotropy of the terbium ions which are slightly too large. The theory of Ref. 13 predicts singularities, associated with the single-ion anisotropy of the rare-earth subsystem, in the magnetic-field behavior of the sound velocities also, but first and foremost in the longitudinal sound velocities, as one can see from the relations given for them in Ref. 13. However, no substantial anomalies were observed in the magnetic-field dependences of the longitudinal velocities in our experiments (Fig. 9). The strongest variations in the sound velocities as a function of an external magnetic field are observed for transverse sound modes (see Figs. 4–8). Thus, the experimental results attest to the fact that the coupling with the single-ion magnetic anisotropy of the rare-earth subsystem of terbium ferroborate is not the main mechanism by which the magnetic subsystem influences the phonon subsystem of this crystal. Another possible explanation of this discrepancy between the theory and our experiment could be a coupling between the single-ion anisotropy and optical rather than acoustic oscillations in the experimental system.

We shall now analyze how a renormalization as a result of sound waves can influence the behavior of sound velocities and absorption. This has been studied theoretically in a general form in Ref. 14, where it is shown that the change occurring in the sound velocities due to renormalization of the exchange interaction constants of the magnetic subsystem has the form

$$\begin{aligned}
\Delta s &= (\Delta s)_1 + (\Delta s)_2,\\
(\Delta s)_1 &= -[\rho V s (g\mu_B)^4 q^2]^{-1}[2|g_0(\mathbf{q})|^2 (g\mu_B \langle S_0^z \rangle)^2 \chi_0^z\\
&\quad + T\sum_k \sum_{\alpha} |g_k(\mathbf{q})|^2 (\chi_k^{\alpha})^2],\\
(\Delta s)_2 &= -[2\rho V s (g\mu_B)^2 q^2]^{-1}[h_0^2(\mathbf{q})(g\mu_B \langle S_0^z \rangle)^2\\
&\quad + T\sum_k \sum_{\alpha} h_k^{\alpha}(\mathbf{q})\chi_k^{\alpha}],
\end{aligned} \tag{2}$$

where the magnetoelastic coupling coefficients are given by the formula

$$g_k^{\alpha}(\mathbf{q}) = \sum_j e^{ik\mathbf{R}_{ji}}(e^{ik\mathbf{R}_{ji}} - 1)\mathbf{u}_{\mathbf{q}} \frac{\partial J_{ij}^{\alpha}}{\partial \mathbf{R}_i}, \tag{3}$$

where h_k^{α} is defined as

$$h_k^{\alpha} = \sum_j e^{-ik\mathbf{R}_{ji}}(e^{ik\mathbf{R}_{ji}} - 1)(e^{-ik\mathbf{R}_{ji}} - 1)\mathbf{u}_{\mathbf{q}}\mathbf{u}_{\mathbf{q}-1} \frac{\partial^2 J_{ij}^{\alpha}}{\partial \mathbf{R}_i \partial \mathbf{R}_j}. \tag{4}$$

In these formulas V is the volume of the crystal, g and μ_B are at the g factor and the Bohr magneton, J_{ij}^{α} are the exchange interaction integrals between the sites i and j, $\alpha = x, y, z$, $\mathbf{R}_{ji}$ is the radius vector of the site i, $\mathbf{R}_{ji}$ is the vector connecting the sites j and i, $\mathbf{q}$ is the wave vector of the sound wave (q is its modulus), $\mathbf{u}_{\mathbf{q}}$ is the polarization factor of the sound wave, $\langle S_0^z \rangle$ is the average moment at one site, and χ_0^{α} is the uniform and χ_k^{α} the nonuniform magnetic susceptibility. In the relations (2) a change of the sound velocity appears as a result of the dynamical coupling between the spin subsystem and the acoustic phonon branches. It is evident from these relations that the change in the magnitude of the sound velocity is proportional to the squared magnetization. Since the magnetization of the system undergoes a jump at the critical field of the spin-reorientation (spin-flop) transition, as one can see from our experiments (see Figs. 4–8) the velocities of sound waves also undergo a jump in this critical field. On the other hand, since the magnetization of the antiferromagnetic system vanishes at $T = T_N$, according to the relations (2) the sound velocities show a very weak singularity at this point, which is in fact observed experimentally (see Fig. 3). It follows from the relations (3) and (4) that the largest changes of the sound velocity should occur for longitudinal sound waves. As one can see from Fig. 9, this does not happen. Such behavior of the sound velocities probably attests to the fact that in terbium ferroborate the exchange interaction between the iron ions is not a direct interaction (along chains) but rather an indirect interaction, which is stronger for interaction with transverse sound modes. It was also found in

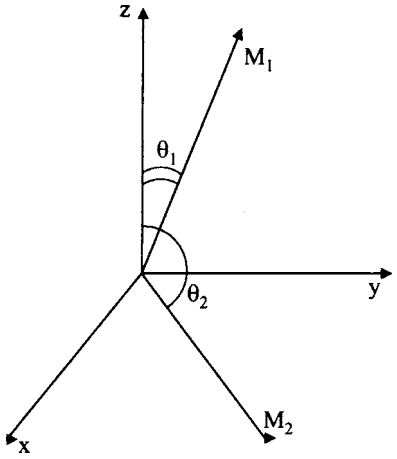

FIG. 10. Illustration of the two-sublattice model of an antiferromagnet.

Ref. 14 how the absorption of sound waves is related with the change of the exchange integrals between magnetic ions. It was shown that this absorption is actually proportional to the change of the sound velocities but multiplied by the ratio of the relaxation rate of the magnetic oscillations to the squared sound speed. The fact that the singularities which we observed in the temperature and magnetic field behavior of absorption are much weaker than the analogous singularities in the behavior of the sound speeds shows that apparently the relaxation rate of the magnetic oscillations is less than sound speeds in terbium ferroborate.

We shall now examine as an alternative to the theoretical description of our experimentally observed singularities a very simple phenomenological model of a two-sublattice easy-axis antiferromagnet interacting with an elastic subsystem.

The expression for the energy of the system has the form

$$F = A(\mathbf{M}_1\mathbf{M}_2) - \frac{K}{2M_0^2}[(M_1^z)^2 + (M_2^z)^2] - \mathbf{H}(\mathbf{M}_1 + \mathbf{M}_2) + B_1 u_{xy}(M_1^x M_2^y + M_1^y M_2^x) + B_2 u_{xy}(M_1^x M_1^y + M_2^x M_2^y) + 2C_{66}u_{xy}^2. \quad (5)$$

Here A is the exchange constant of the antiferromagnetic intersublattice interaction, K is the easy-axis magnetic anisotropy constant ($K,A>0$), B_1 and B_2 are the magnetoelastic interaction constants, and u_{xy} is the deformation in the xy plane. Let the magnetic field $\mathbf{H}$ be oriented along the $\mathbf{z}$ axis, and let the sublattice magnetizations $\mathbf{M}_1$ and $\mathbf{M}_2$ make with this axis the angles θ_1 and θ_2, respectively (see Fig. 10). Let $AM_0=H_E$, $K=M_0H_A$, $B_{1,2}=M_0H_{B1,2}$, where M_0 is the magnetic moment of the sublattice. We shall find the minimum of the energy F with respect to θ_1, θ_2, and u_{xy}, assuming that $B_1, B_2 < A, K, H$. Then there are three possible configurations for the ground state of the magnetic subsystem:

1) antiferromagnetic phase (AF), here $\theta_2=\pi-\theta_1$;
2) spin-flop phase (SF), here $\theta=-\theta_1$;
3) paraphrase, here $\theta_2=\theta_1$.

The energy in the AF phase has the form

$$F = M_0[-H_E\cos 2\theta_1 + H_A \sin^2\theta_1 + 2(H_{B1} + H_{B2})u_{xy}\sin^2\theta_1] + 2C_{66}u_{xy}^2. \quad (6)$$

In the SF phase

$$F = M_0[H_E\cos 2\theta_1 + H_A \sin^2\theta_1 - 2H\cos\theta_1 + 2(H_{B1} - H_{B2})u_{xy}\sin^2\theta_1] + 2C_{66}u_{xy}^2. \quad (7)$$

We shall find the renormalization of the elastic modulus C_{66} due to the interaction with the magnetic subsystem:

$$C_{66}^* = C_{66} - \left\{ \frac{\left(\frac{\partial^2 F}{\partial u_{xy}\partial\theta_1}\right)^2}{\frac{\partial^2 F}{\partial\theta_1^2}} \right|_{\theta_1=\theta_{1\text{eq.}}},$$

where the equilibrium value of θ_1 in the corresponding phase is used:

$\theta_1=0$ in the AF phase and $\cos\theta_1=H/(2H_E-H_A)$ in the SF phase.

In the AF phase we have $C_{66}^*=C_{66}$, i.e. the modulus of C_{66} in this phase remains unchanged. In the SF phase we obtain

$$C_{66}^* = C_{66} - \frac{8(H_{B1}-H_{B2})^2H^2}{(2H_E-H_A)^3}\frac{1-\frac{H^2}{(2H_E-H_A)^2}}{1-\frac{H^2}{(2H_E+H_A)^2}} \approx C_{66} - \frac{(H_{B1}-H_{B2})^2H^2}{H_E^3}. \quad (8)$$

Thus, in the SF phase the elastic modulus C_{66} changes abruptly at the spin-flop transition field. We note that the critical field H_2, below which the AF phase is table, equals $\sqrt{(2H_E+H_A)H_A}$, and the field H_1 above which the SF phase is stable equals $\sqrt{(2H_E-H_A)H_A}/(2H_E+H_A)$, so that a first-order phase transition occurs at $H_{SF}=\sqrt{H_1H_2}=\sqrt{H_A(2H_E-H_A)}$.

It follows from Fig. 7a that the behavior of the modulus C_{66} corresponds to the simple phenomenological model proposed above.

The model for renormalization of the modulus C_{44} is analyzed similarly, but for this model it is necessary to take account of the weak effects of the elastic subsystem on the configuration of the magnetic moments in the ground state.

The observation of hysteresis (i.e. a first-order transition) for small angles of deviation of the direction of the magnetic field from the $\mathbf{z}$ axis corresponds completely to the results of the theoretical analyses.[15]

Hysteresis phenomena, which were observed in the behavior of certain transverse velocities of sound for $H>H_{SF}$ (Figs. 6 and 7) can be explained by the presence of domain structure in the intermediate state of the antiferromagnetic system under study.[16] We note that magneto-optical investigations of a terbium ferroborate single crystal have revealed

the presence of domain structure in the intermediate state near the spin-flop transition.[17]

V. CONCLUSIONS

In summary, the following conclusions can be drawn from the measurements of the magnetic field and temperature dependences of the sound velocity and absorption in terbium ferroborate. In the first place, apparently, magnetoelastic coupling is manifested most strongly in this material not as a result of the influence of displacements of nonmagnetic neighbors (ligands) of rare-earth ions, as previously thought, but rather as a result of the renormalization of the exchange interaction between iron ions, and this interaction is not direct but rather indirect. The magnetic field behavior of the transverse sound modes is described well within the framework of a phenomenological model of two sublattices of iron ions interacting with the elastic vibrations of the lattice.

In the second place, the relaxation rate of magnetic excitations in this system is weaker than in other systems with magnetoelastic coupling (see, for example, Ref. 16), as a result of which sound absorption reflects the special nature of the magnetic system under study more weakly than does the behavior of the sound velocity.

Finally, the domain structure of terbium ferroborate, which exists in an intermediate state, is probably manifested in the hysteresis which was observed in the magnetic field behavior of certain transverse sound velocities in fields above the spin-flop transition field.

We thank V. D. Fil', V. A. Bedarev, A. N. Vasil'ev, and N. P. Kolmakova, for a discussion of the results obtained in the present work and for valuable remarks.

[a)]E-mail: zvyagina@ilt.kharkov.ua

[1]D. Jaque, J. Alloys Compd. **323–324**, 204 (2001).
[2]M. Huang, Y. Chen, and X. Chen, Opt. Commun. **208**, 163 (2002).
[3]J. A. Campa, C. Cascales, E. Gutierres-Puebla, M. A. Monge, I. Rasines, and C. Ruiz-Valero, Chem. Mater. **9**, 237 (1997).
[4]Y. Hinatsu, Y. Doi, K. Ito, M. Wakeshima, and A. Alemi, J. Solid State Chem. **112**, 438 (2003).
[5]A. K. Zvezdin, S. S. Krotov, A. M. Kadorntseva, G. P. Vorob'ev, Yu. F. Popov, A. P. Pyatakov, L. N. Bezmaternykh, and E. A. Popova, JETP Lett. **81**, 272 (2005).
[6]A. K. Zvezdin, G. P. Vorob'ev, A. M. Kadomtseva, Yu. F. Popov, A. P. Pyatakov, L. N. Bezmaternykh, A. V. Kuvardin, and E. A. Popova, JETP Lett. **83**, 509 (2006).
[7]W. A. Dollase and R. J. Reeder, Am. Mineral. **71**, 163 (1986).
[8]A. N. Vasil'ev and E. A. Popova, Fiz. Nizk. Temp. **32**, 968 (2006) [Low Temp. Phys. **32**, 735 (2006)].
[9]D. Fausti, A. A. Nugroho, P. H. M. van Loosdrecht, S. A. Klimin, M. N. Popova, and L. N. Bezmaternykh, Phys. Rev. B **74**, 024403 (2006).
[10]C. Ritter, A. Balaev, A. Vorotynov, G. Petrakovski, D. Velikanov, V. Temerov, and I. Gudim, J. Phys.: Condens. Matter **19**, 196227 (2007).
[11]L. N. Bezmaternykh, V. L. Temerov, I. A. Gudim, and N. A. Stolbovaya, Crystallogr. Rep. **50**, Suppl. 1, 97 (2005).
[12]E. A. Masalitina, V. D. Fil', K. R. Zhekov, A. N. Zholobenko, T. V. Ignatova, and Sing-Ik Lee, Fiz. Nizk. Temp. **29**, 93 (2003) [Low Temp. Phys. **29**, 72 (2003)].
[13]A. A. Demidov, N. P. Kolmakova, L. V. Takunov, and D. V. Volkov, Physica B **398**, 78 (2007).
[14]M. Tachiki and S. Maekawa, Prog. Theor. Phys. **51**, 1 (1974).
[15]M. I. Kaganov and G. K. Chepurnykh, Fiz. Tverd. Tela (Leningrad) **11**, 911 (1969).
[16]V. V. Epemenko and V. A. Sirenko, *Magnetoelastic Properties of Antiferromagnets and Superconductors*, Naukova dumka, Kiev (2004).
[17]V. A. Bedarev, L. N. Bezmaternykh, S. L. Gnatchenko, M. I. Pashchenko, and V. L. Temerov, *Magnetic Intermediate State in the Terbium Iron Borate* $TbFe_3(BO_3)_4$, Proc. MISM-2008, Moscow, June 20–25, 2008.

Translated by M. E. Alferieff